Earth and Planetary Science Letters 369-370 (2013) 169–177

Contents lists available at SciVerse ScienceDirect

Earth and Planetary Science Letters

journal homepage: www.elsevier.com/locate/epsl

Tectonically restricted deep-ocean circulation at the end of the Cretaceous greenhouse

Silke Voigt [a,*], Claudia Jung [a], Oliver Friedrich [a,1], Martin Frank [b], Claudia Teschner [b], Julia Hoffmann [a]

[a] Institute of Geosciences, Goethe-Universität Frankfurt, Altenhöferallee 1, 60439 Frankfurt, Germany
[b] GEOMAR Helmholtz Centre for Ocean Research Kiel, Wischhofstr. 1–3, 24148 Kiel, Germany

ARTICLE INFO

Article history:
Received 22 December 2012
Received in revised form
11 March 2013
Accepted 17 March 2013
Editor: J. Lynch-Stieglitz
Available online 22 April 2013

Keywords:
cretaceous
ocean circulation
neodymium isotopes
gateways

ABSTRACT

The evolution of global ocean circulation toward deep-water production in the high southern latitudes is thought to have been closely linked to the transition from extreme mid-Cretaceous warmth to the cooler Cenozoic climate. The relative influences of climate cooling and the opening and closure of oceanic gateways on the mode of deep-ocean circulation are, however, still unresolved. Here we reconstruct intermediate- to deep-water circulation for the latest Cretaceous based on new high-resolution radiogenic neodymium (Nd) isotope data from several sites and for different water depths in the South Atlantic, Southern Ocean, and proto-Indian Ocean. Our data document the presence of markedly different intermediate water Nd-isotopic compositions in the South Atlantic and Southern Ocean. In particular, a water mass with a highly radiogenic Nd isotope signature most likely originating from intense hotspot-related volcanic activity bathed the crest of Walvis Ridge between 71 and 69 Ma, which formed a barrier that prevented deep-water exchange between the Southern Ocean and the North Atlantic basins. We suggest that the Cenozoic mode of global deep-ocean circulation was still suppressed by tectonic barriers in the latest Cretaceous, and that numerous, mostly regionally-formed and sourced intermediate to deep waters supplied the deep ocean prior to 68 million yr ago.

1. Introduction

The formation of oceanic deep-water masses is the key process for heat transport in the modern ocean-climate system. For the Cretaceous greenhouse world, however, the role of oceanic poleward heat transport as a main driver of long-term climate change has been questioned. Instead, heat transport is thought to have responded to high-latitude cooling due to atmospheric CO_2 reduction (Robinson and Vance, 2012; Robinson et al., 2010). The relationship between the climatic state of the Earth and deep-ocean circulation was in addition affected by the plate tectonic configuration. Due to plate-tectonic limitations and the lack of open seaways between major ocean basins, the formation and circulation of deep-water masses occurred individually in restricted, relatively small oceanic basins over long periods of time in the middle Cretaceous (120–80 Ma; Friedrich et al., 2008; MacLeod et al. 2008, 2011). It is widely assumed that the ongoing opening of the South Atlantic Ocean has connected all major oceanic basins from the early Campanian (~83 Ma) onwards, thus causing a marked change of global ocean circulation (MacLeod et al., 2011; Martin et al., 2012; Murphy and Thomas, 2012; Robinson et al., 2010). The underlying driving mechanisms and source regions of deep-water masses are, however, controversial. It has been suggested that deep waters formed in the North Atlantic (Northern Component Water, NCW) played a significant role in Late Cretaceous ocean circulation (Frank and Arthur, 1999; MacLeod et al., 2011; Martin et al., 2012). Alternatively, the South Atlantic and Indian Ocean domain has been invoked as the main region of deep-water formation, with the sinking of Southern Component Water (SCW) having been a result of early Campanian climate cooling (Brady et al., 1998; Huber et al., 1995; Murphy and Thomas, 2012; Robinson and Vance, 2012; Robinson et al., 2010). Both scenarios imply a transition towards an early Cenozoic mode of deep-ocean circulation mainly driven by sinking of cool waters at high latitudes. In contrast, an alternative hypothesis suggests vertical oceanic mixing at numerous sites via local eddies, which formed as the consequence of weak or missing oceanic fronts related to the lack of permanent polar ice, low hemispheric temperature gradients and weakly developed westerly winds (Hay, 2011).

To resolve the potential influence of different ocean basins during the waning greenhouse climate of the latest Cretaceous, we present new, high-resolution radiogenic Nd isotope records obtained from sedimentary ferromanganese-oxide coatings of three sites in the South Atlantic, the Southern Ocean, and the proto-Indian Ocean (Fig. 1). Nd isotopes can be used as geochemical

* Corresponding author. Tel.: +49 6979840190.
E-mail address: s.voigt@em.uni-frankfurt.de (S. Voigt).
[1] Present address: Institut für Geowissenschaften, Ruprecht-Karls-Universität Heidelberg, Im Neuenheimer Feld 234-236, 69120 Heidelberg, Germany.

0012-821X/$ - see front matter © 2013 Elsevier B.V. All rights reserved.
http://dx.doi.org/10.1016/j.epsl.2013.03.019

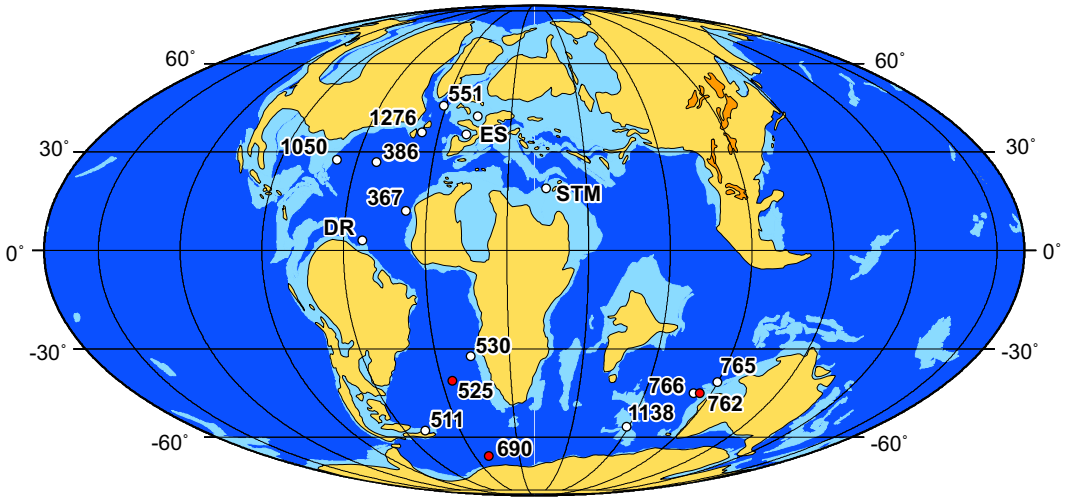

Fig. 1. Palaeogeographic reconstruction at 70 Ma, showing the distribution of shallow shelf seas and ocean basins (map modified from Hay et al. (1999)). The location of DSDP and ODP sites studied here and for which published $\varepsilon_{Nd(t)}$ data exist are indicated with red and white dots, respectively. Abbreviations: DR—Demerara Rise, ES—European shelf, and STM—Southern Tethys margin.

tracer to reconstruct past ocean circulation. The Nd isotope composition of continental rocks is a function of rock type and age, and weathering processes release the Nd to the ocean either via riverine and aeolian input or through exchange processes with shelf sediments (Lacan and Jeandel, 2005). Therefore, water masses are labelled with distinct Nd-isotope compositions in their source regions. Because the oceanic residence time of Nd and the global mixing time of the ocean are similar (e.g. Frank, 2002), the isotopic composition of Nd in seawater, expressed as $\varepsilon_{Nd(t)}$, has been shown to behave quasi-conservatively and thus serves as a tracer for water-mass mixing in the past. Nd isotope signatures of ferromanganese-oxide coatings allow the reconstruction of past deep-water masses at a significantly higher spatial and temporal resolution than commonly achieved by fossil fish debris. Both archives have been shown to generally yield indistinguishable Nd isotope signatures (Martin et al., 2010, 2012). Our Campanian to Maastrichtian Nd isotope data set is augmented by literature data to reconstruct latest Cretaceous (66–76 Ma; Campanian to Maastrichtian) intermediate- to deep-water mass circulation and mixing.

2. Materials and methods

Nd-isotope data have been obtained from three sites in the South Atlantic (Deep Sea Drilling Project [DSDP] Site 525, Walvis Ridge), the Southern Ocean (Ocean Drilling Program [ODP] Site 690, Maud Rise), and the proto-Indian Ocean (ODP Site 762, Exmouth Plateau) (Fig. 1). DSDP Hole 525A is located on top of Walvis Ridge, a volcanic ridge between Africa and the Mid-Atlantic Ridge. During the Maastrichtian, it was situated at 36°S palaeolatitude at a water depth of approximately 1000–1500 m (Li and Keller, 1999; Moore et al., 1984). Maastrichtian stratigraphy of Site 525 is well constrained by palaeomagnetic data (Chave, 1984), as well as by zonations with planktic foraminifera (Li and Keller, 1998) and calcareous nannofossils (Manivit, 1984). Ages of geomagnetic reversals are used as tie-points for the age model (GTS04; Gradstein et al., 2004). In addition, carbon-isotope records of benthic foraminifera (Friedrich et al., 2009; Li and Keller, 1998), globally correlated to other Maastrichtian sites (Voigt et al., 2012), enable a high temporal resolution of inter-site correlation (Fig. 2). The analyzed samples cover the interval of upper chron C32 and chron C31 (488.80–528.57 mbsf, core sections: 44-1/70-71 to 48-2/97-98).

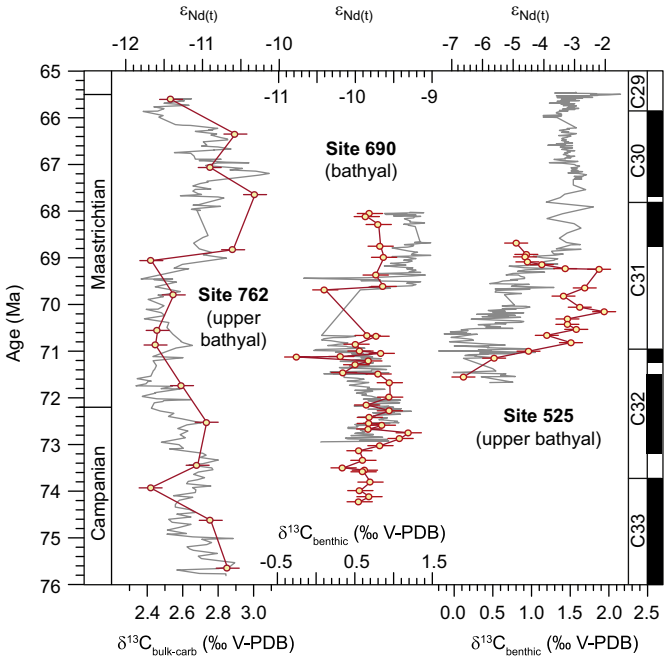

Fig. 2. Radiogenic Nd isotope data obtained from DSDP Site 525 and ODP Sites 762 and 690 (red) relative to carbon isotope variations (grey; Friedrich et al., 2009; Li and Keller, 1998; Thibault et al., 2012). The timescale is the GTS04. The age model is based on biostratigraphically calibrated carbon-isotope correlation (Voigt et al., 2012). Neodymium isotope data are expressed in the $\varepsilon_{Nd(t)}$ notation, which represents the deviation of the measured $^{143}Nd/^{144}Nd$ from that of the Chondritic Uniform Reservoir (Jacobsen and Wasserburg, 1980) in parts per 10,000 and which has been corrected for in-situ production of ^{143}Nd. (For interpretation of the references to color in this figure legend, the reader is referred to the web version of this article.)

ODP Hole 690C recovered uppermost Campanian to Maastrichtian calcareous chalks and oozes on the southwestern flank of Maud Rise, a volcanic ridge located in the eastern Weddell Sea (Barker et al., 1990; Barrera and Savin, 1999) (Fig. 1). The succession was deposited at a palaeolatitude of about 65°S in an estimated water depth of 1800 m (Huber, 1990; Thomas, 1990). The stratigraphy is based on planktonic foraminifera, calcareous nannofossils (Barrera and Huber, 1990; Huber, 1990; Pospichal and Wise, 1990), and palaeomagnetic data (Hamilton, 1990). Ages of geomagnetic reversals are used as tie-points for the age model (GTS04, Gradstein et al., 2004).

A high-resolution benthic foraminiferal carbon-isotope record (Friedrich et al., 2009) enables inter-site correlation to the other sites of this study (Voigt et al., 2012) (Fig. 2). The analyzed samples cover the interval between chrons C32n and C31n (262.32–316.57 mbsf, core sections: 17-1/52-53 to 22-5/47-49).

ODP Hole 762C was drilled in the western part of the central Exmouth Plateau located in the late Cretaceous in the proto-Indian Ocean (Fig. 1). Campanian–Maastrichtian nannofossil chalks were deposited in an upper bathyal setting (<1000 m) at ~43°S palaeolatitude (Zepeda, 1998). The integrated biostratigraphy comprises planktonic foraminifera and calcareous nannofossils (Bralower and Siesser, 1992; Thibault et al., 2012; Zepeda, 1998). Hole 762C has, together with Hole 525A, one of the best defined magnetostratigraphies throughout the upper Campanian–Maastrichtian (Galbrun, 1992). Ages of geomagnetic reversals are used as tie-points for the age model (GTS04; Gradstein et al., 2004). Carbon isotope stratigraphy of bulk-carbonates (Thibault et al., 2012) enables a high-resolution correlation to the other sites of this study (Fig. 2). Data were obtained from the late Campanian magnetochron C33n to the K/Pg boundary (555.04–667.75 mbsf, core sections: 43-1/53-55 to 54-6/64-66).

Radiogenic neodymium isotope data ($\varepsilon_{Nd(t)}$) of the three studied sites were obtained from ferromanganese-oxide coatings of the bulk sediments. Furthermore, to evaluate potential contamination of the seawater Nd-isotope signatures Nd-isotope compositions of the detrital fraction of the sediments were analyzed for a subset of selected samples. In addition, radiogenic $^{87}Sr/^{86}Sr$ ratios were measured on the leached coatings and the detrital fraction of the sediments from all the studied sites (Tables 1 and 2). Nd was extracted from the Fe–Mn oxide coatings following the method of Gutjahr et al. (2007). Approximately 6 g of dry sediment was rinsed 3x with de-ionized water (MQ). 20 ml of a 15% acetic acid/Na acetate buffer was added several times and shaken overnight to remove carbonate. Subsequently, the samples were triple rinsed with de-ionized water. Decarbonated samples were leached with a 0.05 M hydroxylamine hydrochloride (HH)/15%-acetic acid solution (1:1 mixture of MQ:HH), buffered to pH 3.6 with NaOH. The supernatant was pipetted off after centrifugation, dried and redissolved in 0.5 ml 1 M HCl for further chemical treatment. The detrital fraction was rinsed $3\times$ with de-ionized water and dried and ~50 mg was dissolved in a mixture of concentrated HNO_3 and HF and was subsequently dried and redissolved in 0.5 ml 1 M HCl. All samples were passed through a sequence of ion-exchange columns following published standard procedures. Strontium and the REEs were separated using a first cation-exchange step, during which most of the Ba was also removed. A second and third column used 50 μl Sr-Spec resin to separate Sr from Rb (Horwitz et al., 1992) and Ln-Spec resin to separate Nd from Ba and other REEs, respectively (Barrat et al., 1996; Cohen et al., 1988; Le Fèvre and Pin, 2005).

Nd- and Sr-isotopes were analyzed on a Nu Plasma Multicollector-Inductively Coupled Plasma-Mass Spectrometer at GEOMAR Helmholtz Centre for Ocean Research Kiel. For the measurements the samples were dissolved in 2% HNO_3 and diluted to the same concentrations as the standards during the same session. Measured $^{143}Nd/^{144}Nd$ ratios were mass-fractionation corrected to $^{146}Nd/^{144}Nd=0.7219$ and then normalized to the accepted value of the JNdi-1 Nd-isotope standard of 0.512115, which was analyzed after every 6th sample (Tanaka et al., 2000). During this study, repeated measurements of JNdi-1 showed an external long-term reproducibility of $\pm 0.000011(2\sigma)$, which corresponds to $\pm 0.3\varepsilon_{Nd}(2\sigma)$. Procedural Nd blanks were ≤ 25 pg and thus negligible. Measured Nd-isotope ratios were decay corrected to the time of deposition using an average $^{147}Sm/^{144}Nd$ ratio of 0.124 for the coatings and are expressed in the $\varepsilon_{Nd(t)}$ notation (Tables 1 and 2). Measured $^{87}Sr/^{86}Sr$ isotope ratios were mass bias corrected using $^{86}Sr/^{88}Sr=0.1194$ (Steiger and Jäger, 1977). The Sr isotope results were normalized to the accepted value of the NBS987 standard of 0.710245, which was analyzed after every 6th sample. The external long term reproducibility for repeated standard measurements was $\pm 0.000030(2\sigma)$.

3. Results and discussion

3.1. Ferromanganese coatings as archive of past seawater Nd isotope composition

Authigenic ferromanganese coatings of sediment particles acquire bottom-water ε_{Nd} signatures during their early diagenetic

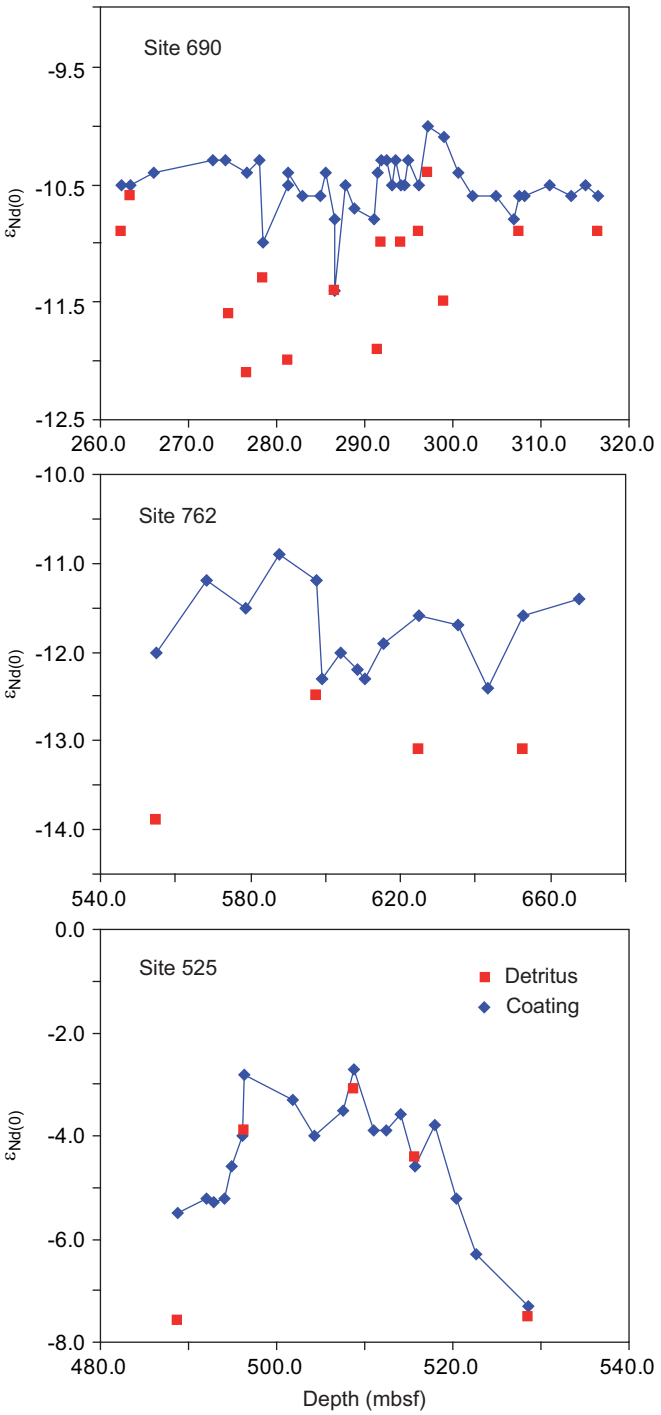

Fig. 3. Comparison of $\varepsilon_{Nd(0)}$ data between ferromanganese coatings (blue) and sediment detritus (red) for the studied sites. (For interpretation of the references to color in this figure legend, the reader is referred to the web version of this article.)

formation near the sediment–water interface and are generally robust to later alteration (Gutjahr et al., 2007; Martin et al., 2010). To evaluate the quality of Nd-isotope data from ferromanganese coatings as archive of the $\varepsilon_{Nd(t)}$ seawater signature, strontium isotope ratios on leached coatings and detritus and neodymium isotopes of the detrital fraction were measured for selected samples (Figs. 3 and 4).

At Sites 690 and 762 the Nd-isotopic composition of detritus reflecting weathering inputs from land is distinctly less radiogenic than that of the coatings. This observation is confirmed by the strontium isotopic composition of detrital fractions which shows a clear shift towards more radiogenic values relative to the contemporaneous seawater strontium isotope evolution (McArthur and Howarth, 2004) (Fig. 4). Detrital fractions of Site 762 are highly radiogenic (>0.7271) typical for weathering supply from old cratonic source rocks and detrital $^{87}Sr/^{86}Sr$ values at Site 690 scatter between 0.7080 and 0.7172 also typical for weathering-derived sources from the surrounding continental landmasses.

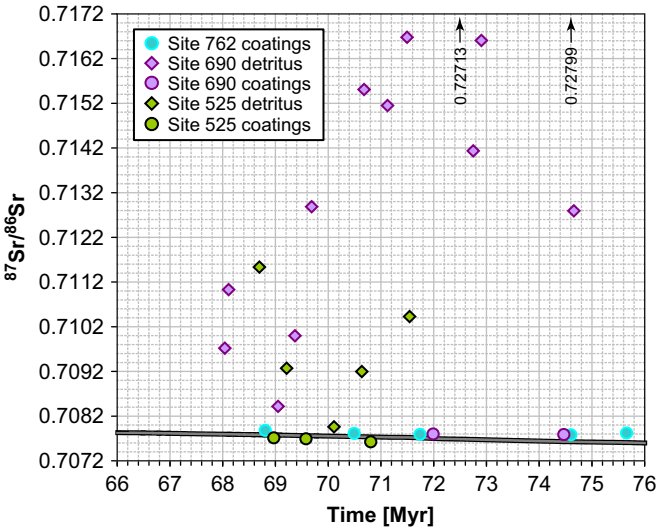

Fig. 4. Plot of $^{87}Sr/^{86}Sr$ ratios of coatings and dissolved detritus relative to the seawater strontium isotope curve (McArthur and Howarth, 2004) (dark grey line). Highly radiogenic strontium isotope data of detritus samples from Site 762 plot outside the diagram. The error bar of Sr isotope data is smaller than the size of symbols.

In contrast, the Nd isotopic composition of detritus and coatings at Site 525 is almost identical and exhibits a highly radiogenic signal with $\varepsilon_{Nd(t)}$ values between –6.6 and –2.0 (Fig. 3). Such a pattern is suspected to originate either from incomplete chemical separation of leached coatings and detrital fractions or from early diagenetic remobilization of REEs from volcanic rocks. The strontium isotopic composition of detrital fractions and leached coatings at Site 525 are clearly different from each other arguing for a small contribution from partial dissolution of the detrital material to the signature extracted from the coatings. While the $^{87}Sr/^{86}Sr$ ratios of the coatings follow the seawater strontium isotope trend within ± 0.0002 (McArthur and Howarth, 2004), the detritus shows a shift towards more radiogenic values typical for continental weathering sources (Fig. 4). This distinct separation provides evidence that (i) the isotopic composition of coatings reflects a seawater signal and that (ii) the isotopic signal of detrital fractions is not significantly affected by residual coatings. Accordingly, the relatively radiogenic $\varepsilon_{Nd(t)}$ values of the leached coatings at Site 525 are considered to reliably represent past seawater signatures at the corresponding water depth (Martin et al. 2010, 2012). Any residual coating may be removable through treatment with stronger chemical reagents but would also start to dissolve detrital minerals causing unwanted alteration of the bulk detrital isotope composition.

3.2. Southern Ocean

The Nd-isotope composition of the Southern Ocean (Maud Rise, Site 690) shows only minor variations (mean value: –9.8; Fig. 2) in

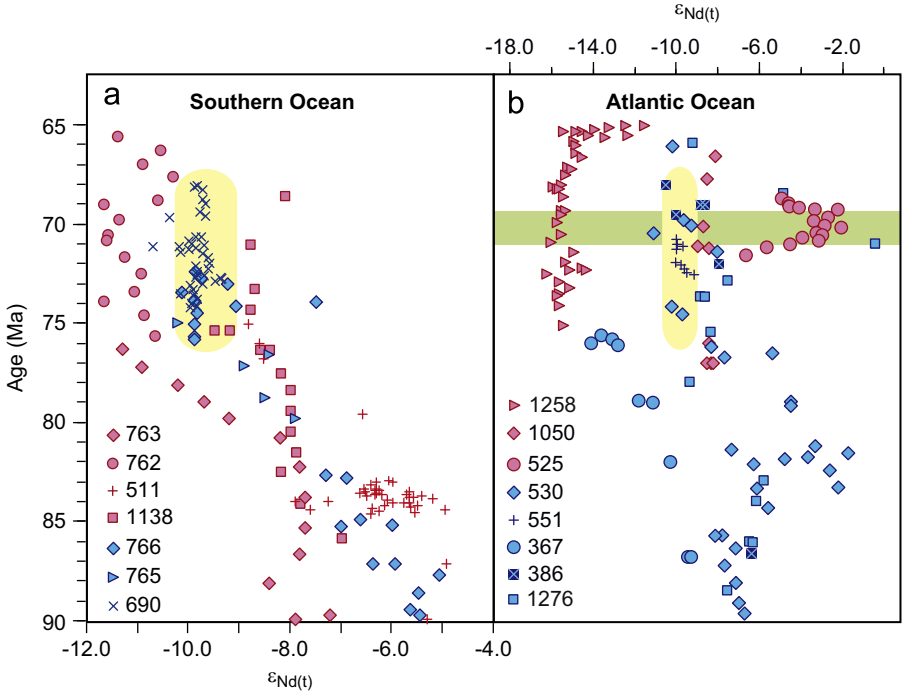

Fig. 5. Late Cretaceous Nd-isotopic composition of bathyal (red) and deep bathyal to abyssal (blue) waters in the Southern Ocean (a) and the Atlantic Ocean (b). The late Campanian to Maastrichtian seawater $\varepsilon_{Nd(t)}$ composition of Southern Component Water (SCW) in the abyssal Southern Ocean is indicated by the yellow field in both diagrams. The green bar marks a period of volcanic activity. Data are from this study (Sites 690, 525 and 762) and from literature (MacLeod et al., 2011; Martin et al., 2010, 2012; Murphy and Thomas, 2012; Robinson et al., 2010; Robinson and Vance, 2012).

late Campanian–Maastrichtian times and is comparable to Palaeocene–Eocene $\varepsilon_{Nd(t)}$ signatures, a time interval when deep waters were clearly formed around Antarctica (Thomas et al., 2003). These $\varepsilon_{Nd(t)}$ values are also similar to those recorded at bathyal and abyssal depths in the proto-Indian Ocean over the past 76 million yr ($\varepsilon_{Nd(t)}$ between −9 and −10; Sites 766, 765 and 1138; Robinson and Vance, 2012; Robinson et al., 2010; Murphy and Thomas, 2012) and indicate that SCW prevailed from the Southern Ocean to the deep proto-Indian Ocean (Fig. 5a). This indicates, that although the Kerguelen Plateau, Broken Ridge and Ninetyeast Ridge formed significant intra-oceanic barriers (Frey et al., 2000), deep-water exchange was maintained by seaways between these morphological highs.

Nd-isotope signatures at the upper bathyal Site 762 were less radiogenic (mean: −11.1; Fig. 5a) and are consistent with values recorded from the upper bathyal Site 763 where a prominent decrease from −8 to −11 was recorded between 82 and 76 Ma (Murphy and Thomas, 2012) (Fig. 5a). The $\varepsilon_{Nd(t)}$ values of these shallower sites are distinctly different from the deeper bathyal Sites 690, 765 and 766 ($\varepsilon_{Nd(t)}$=−10.2 and −9.6) (Robinson et al., 2010; Murphy and Thomas, 2012) and suggest the presence of an unradiogenic neodymium source that influenced intermediate-water masses at upper bathyal depths from the Campanian onwards.

3.3. South Atlantic Ocean

The Nd-isotope composition at the ridge crest of Walvis Ridge (Site 525) shows a pronounced radiogenic signature reaching $\varepsilon_{Nd(t)}$ values between −6.6 and −2.0, while deeper (>2000 m) waters north of Walvis Ridge (Site 530; southern Angola Basin) were characterized by $\varepsilon_{Nd(t)}$ signatures between −11 and −8 (Robinson et al., 2010) (Figs. 2 and 5b). The most radiogenic values (mean: −3.1) occur during a ~2 million yr-long interval within magnetochron C31r. Such a radiogenic seawater Nd-isotope signal in the opening South Atlantic Ocean is an unexpected result, since Atlantic waters were generally influenced by the unradiogenic weathering input from the surrounding continents (e.g. Martin et al., 2012; Puceat et al., 2005; Robinson and Vance, 2012) via dissolved Nd input from rivers and groundwater, as well as partial dissolution of wind-transported particles and by vertical and horizontal mixing by currents (Frank, 2002; Goldstein and Hemming, 2003). Thus, the radiogenic seawater signature at Site 525 requires an alternative origin with a highly radiogenic Nd isotope signature. Possible sources are either (i) early diagenetic remobilization of rare earth elements (REE) from volcanic rocks and sediments, (ii) increased input and leaching of volcanic ash, and/or (iii) boundary exchange between water and sediment particles with radiogenic Nd-isotope composition.

The first mechanism is unlikely because layers rich in volcanic particles were carefully avoided during sampling, and $^{87}Sr/^{86}Sr$ values of the detrital sediment fraction indicate a non-volcanic terrigeneous weathering source (see discussion above, Fig. 4).

In Campanian–Maastrichtian times, the Walvis Ridge was an emerging volcanic structure formed during the passage of South Atlantic oceanic crust over the Tristan hotspot (Torsvik et al., 2006, 2009). Although contributions from volcanic ash do not significantly affect deep-water budgets today (Lacan and Jeandel, 2005), aeolian input and partial dissolution of Nd from volcanic ash may have had an important influence on the isotopic composition of waters at the crest of Walvis Ridge because of its relatively shallow upper bathyal depth. The new data from Site 525 provide evidence for a period of intense volcanic activity between 71 and 69 Ma with a highly radiogenic Nd input into the Atlantic Ocean. Although not well constrained because of the scarcity of data, volcanic radiogenic Nd inputs may also have affected abyssal waters in the North Atlantic (Site 1276) (Fig. 5b; Robinson and Vance, 2012). Similar effects on seawater ε_{Nd} were recently described from the Indian Ocean during the Miocene, where pulses of increased hotspot activity occurred between 20 and 15 Ma ago (Le Houedec et al., 2012).

In addition, the radiogenic Nd isotope signature could have been acquired by exchange of seawater Nd with sediment and rock particles (boundary exchange), through which seawater Nd isotope values can be altered by 3–10 ε_{Nd} units (Lacan and Jeandel, 2005). This process is important for the signatures of ocean-boundary currents today. At Walvis Ridge, the leaching of settled volcanic particles may have additionally contributed to the radiogenic Nd-isotope signature of the ambient deep waters, an argument that is supported by the similarity of $\varepsilon_{Nd(t)}$ values in the leached coatings and detrital fractions of the sediment (Fig. 3). As a consequence of both boundary exchange and leaching of volcanic ash within the water column, the occurrence of radiogenic $\varepsilon_{Nd(t)}$ values on top (Site 525) of Walvis Ridge suggests that water masses on top of Walvis Ridge acquired a distinct regional Nd signature (Walvis Ridge Water—WRW) that persisted for at least 2 million yr during the latest Cretaceous.

3.4. Rio Grande Rise–Walvis Ridge

Palaeobathymetric information (Müller et al., 2008) indicates the presence of intra-oceanic barriers and suggests a clear separation of the North and South Atlantic basins by the Rio-Grande/Walvis Ridge System (RWS; Fig. 6) during the late Campanian to Maastrichtian. The RWS is therefore a critical location to track past changes in deep-water contributions from the Southern Ocean and the North Atlantic, the subsidence of which was proposed to have allowed deep-water exchange either since the mid-Maastrichtian (Frank and Arthur, 1999) or since the early Campanian (Robinson and Vance, 2012).

Our data, in contrast, strongly suggest that the RWS played a crucial role in separating the North and South Atlantic basins at least until the late Maastrichtian. The emergence of the radiogenic Nd source observed at Site 525 changed the regional ε_{Nd} signal of seawater at intermediate water depths on top of the RWS significantly towards radiogenic values. In general, the radiogenic $\varepsilon_{Nd(t)}$ signal at Site 525 can be considered a local signal controlled by local inputs of ash and leaching of volcanic material in the sediment (boundary exchange). The prevalence of a local volcanic source is also supported by the $\varepsilon_{Nd(t)}$ record at the northern flank of Walvis Ridge (Site 530; Robinson et al., 2010). Although situated at abyssal depths, similarly radiogenic seawater ε_{Nd} values were recorded between 78 and 83 Ma (Fig. 7) and coincided with an interval of frequent deposition of turbidites rich in volcanoclastic material (Hay et al., 1984). Turbidite activity vanished in late Campanian to Maastrichtian times resulting in a lower reactivity of sediments for boundary exchange and the prevalence of unradiogenic seawater ε_{Nd} signatures at abyssal depths.

Consequently, the available data show that different water masses with distinct $\varepsilon_{Nd(t)}$ signatures concomitantly occurred on top and in abyssal depths on the northern flank of Walvis Ridge during the Maastrichtian. Any water mass (like e.g. the SCW) that may have flowed across the Walvis Ridge would have experienced a modification of its Nd-isotopic composition to significantly more radiogenic values. The distinctly unradiogenic signatures of Site 530 in the Angola Basin show that the Walvis Ridge served as an effective barrier for deep-water flow at this time (Robinson et al., 2010). Deep waters north of the RWS in the emerging North Atlantic, although similar in Nd-isotopic composition to those of the SCW, must have acquired their Nd from local sources.

It was not before the Palaeocene–Eocene that one single water mass encompassed the entire depth range above Walvis Ridge and was sourced by deep waters from the Southern Ocean (Fig. 7) (Via and

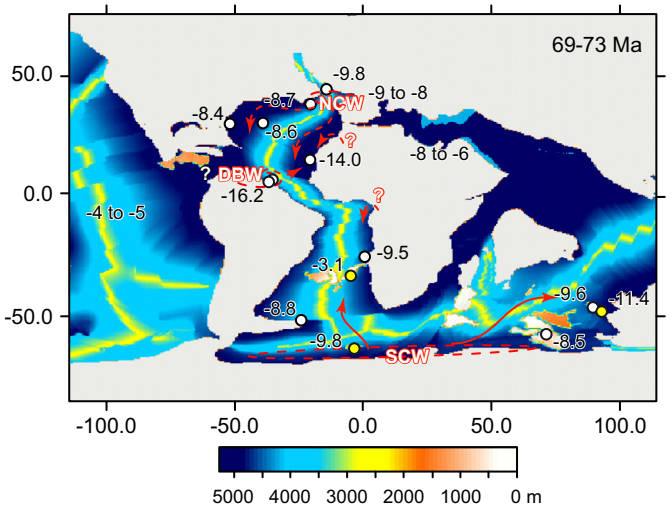

Fig. 6. Palaeobathymetric reconstruction of the Pacific, North- and South Atlantic, Southern and proto-Indian oceans at 71 Ma without shelf seas (data from Müller et al., 2008). Note the lack of shallow seas and the existence of numerous barriers e. g. in the Caribbean. Average intermediate- to deep-water Nd isotope values at different sites and water depths are from the late Campanian to early Maastrichtian (69–73 Ma) interval. Neodymium isotope data are from this study and from Frank et al. (2005), MacLeod et al. (2011), Martin et al. (2012), Puceat et al. (2005), Robinson and Vance (2012), and Robinson et al. (2010). Arrows schematically mark the flow of different deep-water masses reconstructed in this study. NCW—Northern Component Water, and SCW—Southern Component Water.

Thomas, 2006). This observation is supported by studies related to the palaeo-redox conditions of the South Atlantic Ocean based on REE patterns of carbonates deposited on the RWS (Hu et al., 1988; Wang et al., 1986). These authors used Ce anomalies to show that anoxic conditions prevailed in the Angola–Brazil basins until the end of the Maastrichtian and that a sufficient oxidation as a result of improved deep-water circulation due to the subsidence of barriers did not occur before 55–58 Ma ago. Further evidence comes from foraminiferal dissolution data that demonstrate the upwelling of corrosive deep waters at the southern flank of the RWS that were not able to get across this barrier during the latest Maastrichtian (Kucera et al., 1997). Even today, the Angola Basin is relatively isolated and deep waters are dominated by North Atlantic Deep Water modified through exchange with the southwest African margin (Rickli et al., 2009), which is evident from its highly unradiogenic Nd isotope signatures. The northward flow of Antarctic Bottom Water is blocked by the eastern Walvis Ridge (Hay et al. 1984).

Therefore, our new data reveal that the RWS was an effective barrier for deep-water exchange during the latest Cretaceous. We consider it highly unlikely that volumetrically substantial quantities of SCW rose to upper bathyal depths, passed the RWS and subsequently sank again to abyssal depths to drive deep ocean circulation in the Atlantic Ocean north of the barrier. Such fundamental changes in ocean circulation towards a Cenozoic circulation system only occurred later between 65 and 58 Ma. Additional and longer Nd-isotope records are needed from different sites and water depths along the RWS to define the precise timing of the shallowing of the RWS to allow for deep-water flow between the Southern Ocean and the northern Atlantic Ocean in the latest Cretaceous to earliest Cenozoic.

3.5. North Atlantic Ocean and inter-oceanic deep-water connexions

Published North Atlantic deep-water Nd-isotope data exhibit a large range of values in late Campanian–Maastrichtian times. Abyssal and deep bathyal $\varepsilon_{Nd(t)}$ values (−8.5 to −8.7) in the western North Atlantic (Bermuda Rise and Site 1276) were slightly more radiogenic than those recorded for SCW (Figs. 5b, 6, and 7) (Martin et al., 2012; Robinson and Vance, 2012). In contrast, seawater Nd-isotopes in the abyssal eastern North Atlantic (near Cape Verde) are highly unradiogenic ($\varepsilon_{Nd(t)}$ ~−14), an observation which led to the hypothesis that Demerara Bottom Water (DBW) sank into the deeper parts of the Atlantic ocean (Martin et al., 2012). Alternatively, deep waters in the Cape Verde Basin may have been formed locally at sites off West Africa analogous to the mode of DBW formation (Fig. 6). The available data argue for the concomitant presence of different deep-water $\varepsilon_{Nd(t)}$ signatures in the abyssal plains east and west of the mid-ocean ridge and limited deep-water exchange between the deep sub-basins.

The North Atlantic Ocean north of the RWS was still a very narrow ocean at the time. Possible connexions may have existed only across the RWS at bathyal depths, the Caribbean, and/or narrow Tethyan gateways (Fig. 6). An influence of Pacific deep waters entering the deep North Atlantic through the Caribbean Seaway during the late Campanian to Maastrichtian is unlikely due to the restricted nature of the latter at that time and the absence of highly radiogenic $\varepsilon_{Nd(t)}$ signatures of bottom waters in the North Atlantic. Recent plate tectonic reconstructions indicate that the boundary between the Caribbean and the proto-Pacific plate was either formed by a permanent trans-American eastward-dipping subduction zone (Meschede and Frisch, 1998) or by the newly formed Panama–Costa Rica Arc that occurred either during (70 Ma; Seton et al., 2012) or before the accretion of the Caribbean arc to the Bahaman Platform (80–88 Ma; Pindell and Kennan, 2009 or 75–73 Ma; Buchs et al., 2010).

Possible Tethyan gateways became progressively restricted during Maastrichtian times by the northward movement of Africa related to the opening of the South Atlantic Ocean. Tethyan seawater $\varepsilon_{Nd(t)}$ signals are dominated by a shift towards more radiogenic values in Campanian–Maastrichtian times that indicates a stronger influence of Pacific deep waters in the eastern Tethys (Fig. 6) (Frank et al., 2005; Soudry et al., 2006). However, Pacific deep waters did not enter the North Atlantic from the east as indicated by the absence of a radiogenic signature there.

Besides the proposed sinking of DBW (Martin et al., 2012), regional formation of Northern Component Water (NCW) was suggested as an alternative deep-water source (MacLeod et al., 2011; Martin et al., 2012). Such a water mass may have formed in shelf settings of Western Europe and/or North America, from where it flowed into the North Atlantic basin (MacLeod et al., 2011; Martin et al., 2012). Supporting evidence comes from the similarity of deep-sea and shallow-water $\varepsilon_{Nd(t)}$ values around −8 to −9 (Fig. 6) recorded at several North Atlantic sites (Martin et al., 2012; Robinson and Vance, 2012) and European shelf seas (Puceat et al., 2005). However, in contrast to the model of MacLeod et al. (2011), our new data show that deep-water flow of NCW was most likely not able to pass the RWS, and thus failed to be a major driver of deep-ocean circulation. Even though the Central Atlantic Gateway (CAG) gave way to a deep-water connexion between the North and South Atlantic basins at some time between the Cenomanian–Turonian (Tucholke and Vogt, 1979) and the early Campanian (Friedrich and Erbacher, 2006), it may still have formed a barrier in the early Maastrichtian due the emplacement of the large igneous province at Sierra Leone Rise ~73 million yr ago (Torsvik et al., 2006). At present, the spare data base do not allow statements about how far south a possible NCW deep water flow can be traced. Deep-ocean circulation within the North Atlantic prior to 68 Ma was thus most likely influenced by numerous regional water-mass sources, such as DBW (MacLeod et al., 2011), NCW, and other yet unknown deep waters, whereby vertical mixing was likely promoted by local eddies (Hay, 2011) thus contributing to the prevailing highly diverse Nd-isotope signals (−8 to −16; Figs. 5 and 6).

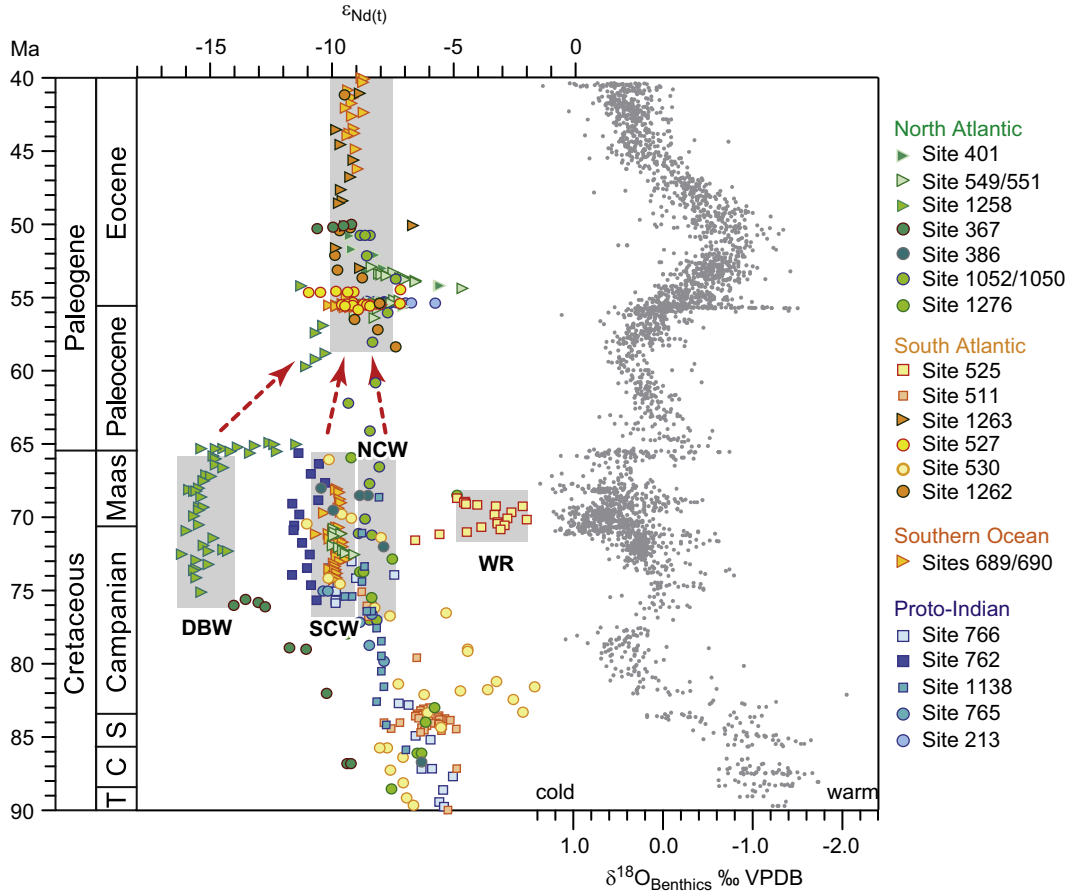

Fig. 7. Comparison of $\varepsilon_{Nd(t)}$ data of different oceanic basins during the Late Cretaceous and early Palaeogene compared to the benthic $\delta^{18}O$ compilation (Friedrich et al., 2012; Zachos et al., 2008). Different water depths are indicated by circles (abyssal, > 2000 m), triangles (deep bathyal, 2000–1500 m) and squares (mid- to upper bathyal, < 1500 m). The timescale is the GTS04. Note the wide range of $\varepsilon_{Nd(t)}$ data in Campanian–Maastrichtian Atlantic Ocean deep and intermediate waters, and the more uniform Nd-isotope composition of Atlantic waters from the Eocene onwards (stippled red arrows). Neodymium isotope data are from this study and from Frank et al. (2005), MacLeod et al. (2008, 2011), Robinson and Vance (2012), Robinson et al. (2010), Thomas et al. (2003), Via and Thomas (2006). SCW—Southern Component Water, DBW—Demerara Bottom Water, and WRW—Walvis Ridge Water.

Extended shelf seas prevailed due to the high sea level until the Maastrichtian. Although the mode of exchange between shelf and oceanic water masses is largely unknown for the Cretaceous, the shelves most likely served as multiple source areas for distinct intermediate waters. Thus, the Nd-isotopic composition at upper bathyal depths of Exmouth Plateau (Site 762) suggests the presence of a water mass that acquired its isotopic signature from contributions of continental sources and was not dense enough to sink to abyssal depths (Fig. 6). Similarly, the Nd-isotope signatures at bathyal sites of the Falkland Plateau (Site 511) (Robinson et al., 2010), Demerara Rise (MacLeod et al., 2008, 2011) and Goban Spur (Martin et al., 2012) differ significantly from those at abyssal sites (Robinson and Vance, 2012), thus predominantly reflecting local weathering contributions from the hinterland.

Modern intermediate and thermocline waters are formed by subduction along the Subtropical and Polar frontal systems forced by the wind stress of the westerly winds (Hay, 2008). The stability of westerly wind forcing is maintained by the polar high pressure cell related to the presence of permanent ice shields today. The situation in the Cretaceous was completely different. The lack of permanent polar ice together with the palaeogeographic constellation of an isolated Arctic ocean, an almost isolated North Atlantic and a narrow South Atlantic might have resulted in seasonally pronounced latitudinal and longitudinal shifts of the atmospheric low and high pressure cells in polar areas and the development of variable wind systems at mid-latitudes (Hay and Flögel, 2012). Hay (2011) proposed a model, in which the instability of the westerly wind system favours the formation of meso-scale eddies instead of oceanic frontal systems. Deep oceanic convection was achieved by down- and upwelling of water masses in anticyclonic and cyclonic eddies. Their position was strongly controlled by the geometry and bathymetry of ocean basins and density differences among water masses were mainly controlled by salinity changes related to the regional balance of evaporation and precipitation. Our compilation of new and available seawater Nd-isotope data clearly shows the broad variety of Late Cretaceous abyssal seawater Nd-isotope signatures. Such a pattern is difficult to maintain under conditions of large scale globally connected deep water convection. Furthermore, the tectonic restrictions in the young Atlantic Ocean inhibited the development of a global thermohaline circulation system encompassing all ocean basins. Although the "Hay Ocean" is only a hypothesis, the growing evidence of distinct seawater Nd-isotopic compositions in different Late Cretaceous sub-basins supports the idea that deep oceanic convection at multiple sites (eddies) of down- and upwelling was a possible mode of deep-water formation for small and restricted ocean basins as the Atlantic Ocean until latest Cretaceous time.

4. Conclusions

Our new late Campanian to Maastrichtian bottom water Nd isotope data reveal multiple, local water sources for nearly every

site investigated, which suggests a circulation system that was fundamentally different from the modern. In particular, the occurrence of a water mass with a radiogenic Nd isotope signature on top of the RWS indicate this structure to have been a barrier for deep-water exchange between the Southern Ocean and North Atlantic basins until the late Maastrichtian. The narrow geometry of the Atlantic Ocean together with tight to closed connexions towards the Tethys and the Pacific Ocean limited volumetrically substantial deep-water exchange and promoted a local mode of deep oceanic convection in the Atlantic. Available Nd isotope data from the North Atlantic indicate the prevalence of different water masses in the abyssal plains and support a mode of ocean circulation that was maintained by down- and upwelling in various meso-scale eddies as proposed by Hay (2011).

Climatic cooling as evident from the benthic $\delta^{18}O$ compilation (Friedrich et al., 2012; Zachos et al., 2008) and the opening of gateways between 83 and 78 Ma may have initiated SCW formation in the southern hemisphere oceans (Robinson and Vance, 2012; Robinson et al., 2010; Martin et al., 2012). However, distinct deep water Nd-isotopic compositions in different Late Cretaceous sub-basins in the young Atlantic Ocean suggest that tectonic restriction instead of climate change controlled deep-water formation there. SCW formation did not drive global ocean circulation before gateway opening and mid-ocean ridge subduction further deepened ocean basins (Müller et al., 2008) between 68 and 58 Ma. These consecutive plate-tectonic events played a crucial role in the global linkage of oceanic deep-water reservoirs and the establishment of a similar to modern global thermohaline circulation system.

Acknowledgements

This research used samples provided by the Deep Sea Drilling Project and the Ocean Drilling Program. ODP has been sponsored by the US National Science Foundation and participating countries under the management of Joint Oceanographic Institutions. We want to thank J. Pross and the reviewers for their insightful comments which helped to improve the scientific discussion of this paper. Financial support for this study was provided by the German Research Foundation DFG (VO687/10-1, VO687/10-2 to S.V., FR2544/2-1 to O.F. and FR1198/7-1 to M.F.).

Appendix A. Supporting information

Supplementary data associated with this article can be found in the online version at http://dx.doi.org/10.1016/j.epsl.2013.03.019.

References

Barker, P.F., Kennett, J.P., et al., 1990. Proc. Ocean Drill. Program: Sci. Results, 113.
Barrat, J.A., Keller, F., Amosse, J., Taylor, R.N., Nesbitt, R.W., Hirata, T., 1996. Determination of rare earth elements in sixteen silicate reference samples by ICP-MS after Tm addition and ion exchange separation. Geostand. Newslett. 20, 133–139.
Barrera, E., Huber, B.T., 1990. Evolution of antarctic waters during the Maestrichtian: foraminifer oxygen and carbon isotope ratios, Leg 113. Proc. Ocean Drill. Program: Sci. Results 113, 813–827.
Barrera, E., Savin, S.M., 1999. Evolution of late Campanian–Maastrichtian marine climates and oceans. In: Barrera, E., Johnson, C. (Eds.), Evolution of the Cretaceous Ocean-Climate System. Geological Society of America, Boulder, pp. 245–282.
Brady, E.C., DeConto, R.M., Thompson, S.L., 1998. Deep water formation and poleward ocean heat transport in the warm climate extreme of the Cretaceous (80 Ma). Geophys. Res. Lett. 25, 4205–4208.
Bralower, T.J., Siesser, W., 1992. Cretaceous calcareous nannofossil biostratigraphy of Sites 761, 762 and 763, Exmouth and Wombat Plateaus, northwest Australia. Proc. Ocean Drill. Program: Sci. Results 122, 529–556.
Buchs, D.M., Arculus, R.J., Baumgartner, P.O., Baumgartner-Mora, C., Ulianov, A., 2010. Late Cretaceous arc development on the SW margin of the Caribbean Plate: insights from the Golfito, Costa Rica, and Azuero, Panama, complexes. Geochem. Geophys. Geosyst. 11, Q07s24, http://dx.doi.org/10.1029/2009gc002901.
Chave, A.D., 1984. Lower Paleocene-Upper Cretaceous magnetostratigraphy, sites 525, 527, 528, and 529, Deep Sea Drilling Project Leg 74. Deep Sea Drill. Program Initial Rep. 74, 525–532.
Cohen, A.S., Onions, R.K., Siegenthaler, R., Griffin, W.L., 1988. Chronology of the pressure–temperature history recorded by a granulite terrain. Contrib. Mineral. Petrol. 98, 303–311.
Frank, M., 2002. Radiogenic isotopes: tracers of past ocean circulation and erosional input. Rev. Geophys. 40, 1001, http://dx.doi.org/10.1029/2000RG000094.
Frank, T.D., Arthur, M.A., 1999. Tectonic forcings of Maastrichtian ocean-climate evolution. Paleoceanography 14, 103–117.
Frank, T.D., Thomas, D.J., Leckie, R.M., Arthur, M.A., Bown, P.R., Jones, K., Lees, J.A., 2005. The Maastrichtian record from Shatsky Rise (northwest Pacific): a tropical perspective on global ecological and oceanographic changes. Paleoceanography 20, PA 1008, http://dx.doi.org/10.1029/2004PA001052.
Frey, F.A., Coffin, M.F., Wallace, P.J., Weis, D., Zhao, X., Wise, S.W., Wahnert, V., Teagle, D.A.H., Saccocia, P.J., Reusch, D.N., Pringle, M.S., Nicolaysen, K.E., Neal, C. R., Muller, R.D., Moore, C.L., Mahoney, J.J., Keszthelyi, L., Inokuchi, H., Duncan, R. A., Delius, H., Damuth, J.E., Damasceno, D., Coxall, H.K., Borre, M.K., Boehm, F., Barling, J., Arndt, N.T., Antretter, M., 2000. Origin and evolution of a submarine large igneous province: the Kerguelen Plateau and Broken Ridge, southern Indian Ocean. Earth Planet. Sci. Lett. 176, 73–89.
Friedrich, O., Erbacher, J., 2006. Benthic foraminiferal assemblages from Demerara Rise (ODP Leg 207, western tropical Atlantic): possible evidence for a progressive opening of the Equatorial Atlantic Gateway. Cretaceous Res. 27, 377–397.
Friedrich, O., Erbacher, J., Moriya, K., Wilson, P.A., Kuhnert, H., 2008. Warm saline intermediate waters in the Cretaceous tropical Atlantic Ocean. Nat. Geosci. 1, 453–457.
Friedrich, O., Herrle, J.O., Wilson, P.A., Cooper, M.J., Erbacher, J., Hemleben, C., 2009. Early Maastrichtian carbon cycle perturbation and cooling event: implications from the South Atlantic Ocean. Paleoceanography 24, PA2211, http://dx.doi.org/10.1029/2008PA001654.
Friedrich, O., Norris, R.D., Erbacher, J., 2012. Evolution of middle to Late Cretaceous oceans-A 55 m.y. record of Earth's temperature and carbon cycle. Geology 40, 107–110.
Galbrun, B., 1992. Magnetostratigraphy of Upper Cretaceous and lower Tertiary sediments, Sites 761 and 762, Exmouth Plateau, northwest Australia. Proc. Ocean Drill. Program: Sci. Results 122, 699–716.
Gradstein, F., Ogg, J., Smith, A., 2004. A Geologic Time Scale. Cambridge University Press, Cambridge.
Goldstein, S.L., Hemming, S.H., 2003. Long lived isotopic tracers in oceanography, paleoceanography, and ice sheet dynamics. In: Elderfield, H. (Ed.), Treatise on geochemistry, vol. 17, New York, Elsevier, pp. 453–489.
Gutjahr, M., Frank, M., Stirling, C.H., Klemm, V., van de Flierdt, T., Halliday, A.N., 2007. Reliable extraction of a deepwater trace metal isotope signal from Fe–Mn oxyhydroxide coatings of marine sediments. Chem. Geol. 242, 351–370.
Hamilton, N., 1990. Mesozoic magnetostratigraphy of Maud Rise, Antarctica. Proc. Ocean Drill. Program: Sci. Results 113, 255–260.
Hay, W.W., 2008. Evolving ideas about the Cretaceous climate and ocean. Cretaceous Res. 29, 725–753.
Hay, W.W., 2011. Can humans force a return to a 'Cretaceous' climate? Sedim. Geol. 235, 5–26.
Hay, W.W., Flögel, S., 2012. New thoughts about Cretaceous climate and oceans. Earth-Sci. Rev. 115, 262–272.
Hay, W.W., Sibuet, J.-C., the Shipboard Scientific Party, 1984. Site 530: southeastern corner of the Angola Basin. Deep Sea Drill. Proj. Initial Rep. 75, 20–285.
Hay, W.W., DeConto, R.M., Wold, C.N., Wilson, K.M., Voigt, S., Schulz, M., Rossby Wold, A., Dullo, C., Ronov, A.B., Balukhovsky, A.N., Söding, E., 1999. Alternative global Cretaceous paleogeography. In: Barrera, E., Johnson, C.C. (Eds.), Evolution of the Cretaceous Ocean-Climate System. Boulder, Colorado, pp. 1–47.
Horwitz, E.P., Chiarizia, R., Dietz, M.L., 1992. A novel strontium-selective extraction chromatographic resin. Solvent Extr. Ion Exch. 10, 313–336.
Hu, X., Wang, Y.L., Schmitt, R.A., 1988. Geochemistry of sediments on the Rio-Grande-Rise and the redox evolution of the South-Atlantic Ocean. Geochim. Cosmochim. Acta 52, 201–207.
Huber, B.T., 1990. Maestrichtian planktonic foraminifer biostratigraphy of the Maud Rise (Weddell Sea, Antarctica): ODP Leg 113 Holes 689B and 690C. Proc. Ocean Drill. Program: Sci. Results 113, 489–513.
Huber, B.T., Hodell, D.A., Hamilton, C.P., 1995. Middle–Late Cretaceous climate of the southern high latitudes: stable isotopic evidence for minimal equator-to-pole thermal gradients. Geol. Soc. Am. Bull. 107, 1164–1191.
Jacobsen, S.B., Wasserburg, G.J., 1980. Sm–Nd isotopic evolution of chondrites. Earth Planet. Sci. Lett. 50, 139–155.
Kucera, M., Malmgren, B.A., Sturesson, U., 1997. Foraminiferal dissolution at shallow depths of the Walvis Ridge and Rio Grande rise during the latest Cretaceous: inferences for deep-water circulation in the South Atlantic. Palaeogeogr. Palaeoclimatol. Palaeoecol. 129, 195–212.
Lacan, F., Jeandel, C., 2005. Neodymium isotopes as a new tool for quantifying exchange fluxes at the continent–ocean interface. Earth Planet. Sci. Lett. 232, 245–257.
Le Fèvre, B., Pin, C., 2005. A straightforward separation scheme for concomitant Lu–Hf and Sm–Nd isotope ratio and isotope dilution analysis. Anal. Chim. Acta 543, 209–221.

Le Houedec, S., Meynadier, L., Allègre, C.J., 2012. Nd isotope systematics on ODP Sites 756 and 762 sediments reveal major volcanic, oceanic and climatic changes in South Indian Ocean over the last 35 Ma. Earth Planet. Sci. Lett. 327–328, 29–38.
Li, L., Keller, G., 1998. Maastrichtian climate, productivity and faunal turnovers in planktic foraminifera in South Atlantic DSDP Site 525A and 21. Mar. Micropaleontol. 33, 55–86.
Li, L., Keller, G., 1999. Variability in Late Cretaceous climate and deep waters: evidence from stable isotopes. Mar. Geol. 161, 171–190.
MacLeod, K.G., Londono, C.I., Martin, E.E., Berrocoso, A.J., Basak, C., 2011. Changes in North Atlantic circulation at the end of the Cretaceous greenhouse interval. Nat. Geosci. 4, 779–782.
MacLeod, K.G., Martin, E.E., Blair, S.W., 2008. Nd isotopic excursion across Cretaceous ocean anoxic event 2 (Cenomanian–Turonian) in the tropical North Atlantic. Geology 36, 811–814.
Manivit, H., 1984. Paleogene and Upper Cretaceous calcareous nannofossils from Deep Sea Drilling Project Leg 74. Initial Rep. Deep Sea Drill. Program 74, 475–499.
Martin, E.E., Blair, S.W., Kamenov, G.D., Scher, H.D., Bourbon, E., Basak, C., Newkirk, D.N., 2010. Extraction of Nd isotopes from bulk deep sea sediments for paleoceanographic studies on Cenozoic time scales. Chem. Geol. 269, 414–431.
Martin, E.E., MacLeod, K.G., Berrocoso, A.J., Bourbon, E., 2012. Water mass circulation on Demerara Rise during the Late Cretaceous based on Nd isotopes. Earth Planet. Sci. Lett. 327, 111–120.
McArthur, J.M., Howarth, R.J., 2004. Strontium isotope stratigraphy. In: Gradstein, F. M., Ogg, J.G., Smith, A.G. (Eds.), A Geologic Time Scale 2004. Cambridge University Press, Cambridge, pp. 96–105.
Meschede, M., Frisch, W., 1998. A plate-tectonic model for the Mesozoic and Early Cenozoic history of the Caribbean plate. Tectonophysics 296, 269–291.
Moore Jr, T.C., Rabinowitz, P.D., et al., 1984. Site 525. Initial Rep. Deep Sea Drill. Program 74, 41–160.
Müller, R.D., Sdrolias, M., Gaina, C., Steinberger, B., Heine, C., 2008. Long-term sea-level fluctuations driven by ocean basin dynamics. Science 319, 1357–1362.
Murphy, D.P., Thomas, D.J., 2012. Cretaceous deep-water formation in the Indian sector of the Southern Ocean. Paleoceanography 27, PA1211, http://dx.doi.org/10.1029/2011PA002198.
Pindell, J.L., Kennan, L., 2009. Tectonic evolution of the Gulf of Mexico, Caribbean and northern South America in the mantle reference frame: an update. In: James, K.H., Lorente, M.A., Pindell, J.L. (Eds.), The origin and evolution of the Caribbean Plate, Geological Society, London, Special Publication 328, pp. 1–55.
Pospichal, J.J., Wise, S.W., 1990. Maestrichtian calcareous nannofossil biostratigraphy of the Maud Rise, ODP Leg 113 Sites 689 and 690, Weddell Sea. Proc. Ocean Drill. Program: Sci. Results 113, 465–487.
Puceat, E., Lecuyer, C., Reisberg, L., 2005. Neodymium isotope evolution of NW Tethyan upper ocean waters throughout the Cretaceous. Earth Planet. Sci. Lett. 236, 705–720.
Rickli, J., Frank, M., Halliday, A.N., 2009. The hafnium-neodymium isotopic composition of Atlantic seawater. Earth Planet. Sci. Lett. 280, 118–127.
Robinson, S.A., Murphy, D.P., Vance, D., Thomas, D.J., 2010. Formation of "Southern Component Water" in the Late Cretaceous: evidence from Nd-isotopes. Geology 38, 871–874.
Robinson, S.A., Vance, D., 2012. Widespread and synchronous change in deep-ocean circulation in the North and South Atlantic during the Late Cretaceous. Paleoceanography 27, PA1102, http://dx.doi.org/10.1029/2011PA002240.
Seton, M., Müller, R.D., Zahirovic, S., Gaina, C., Torsvik, T., Shephard, G., Talsma, A., Gurnis, M., Turner, M., Maus, S., Chandler, M., 2012. Global continental and ocean basin reconstructions since 200 Ma. Earth-Sci. Rev. 113, 212–270.
Soudry, D., Glenn, C.R., Nathan, Y., Segal, I., VonderHaar, D., 2006. Evolution of Tethyan phosphogenesis along the northern edges of the Arabian–African shield during the Cretaceous–Eocene as deduced from temporal variations of Ca and Nd isotopes and rates of P accumulation. Earth-Sci. Rev. 78, 27–57.
Steiger, R.H., Jäger, E., 1977. Subcommission on Geochronology—convention on use of decay constants in geochronology and cosmochronology. Earth Planet. Sci. Lett. 36, 359–362.
Tanaka, T., Togashi, S., Kamioka, H., Amakawa, H., Kagami, H., Hamamoto, T., Yuhara, M., Orihashi, Y., Yoneda, S., Shimizu, H., Kunimaru, T., Takahashi, K., Yanagi, T., Nakano, T., Fujimaki, H., Shinjo, R., Asahara, Y., Tanimizu, M., Dragusanu, C., 2000. JNdi-1: a neodymium isotopic reference in consistency with LaJolla neodymium. Chem. Geol. 168, 279–281.
Thibault, N., Husson, D., Harlou, R., Gardin, S., Galbrun, B., Huret, E., Minoletti, F., 2012. Astronomical calibration of upper Campanian–Maastrichtian carbon isotope events and calcareous plankton biostratigraphy in the Indian Ocean (ODP Hole 762C): implication for the age of the Campanian–Maastrichtian boundary. Palaeogeogr. Palaeoclimat. Palaeoecol. 337, 52–71.
Thomas, D.J., Bralower, T.J., Jones, C.E., 2003. Neodymium isotopic reconstruction of late Paleocene–early Eocene thermohaline circulation. Earth Planet. Sci. Lett. 209, 309–322.
Thomas, E., 1990. Late Cretaceous through Neogene deep-sea benthic foraminifers (Maud Rise, Weddell Sea Antarctica). Proc. Ocean Drill. Program: Sci. Results 113, 571–594.
Torsvik, T.H., Rousse, S., Labails, C., Smethurst, M.A., 2009. A new scheme for the opening of the South Atlantic Ocean and the dissection of an Aptian salt basin. Geophys. J. Int. 177, 1315–1333.
Torsvik, T.H., Smethurst, M.A., Burke, K., Steinberger, B., 2006. Large igneous provinces generated from the margins of the large low-velocity provinces in the deep mantle. Geophys. J. Int. 167, 1447–1460.
Tucholke, B.E., Vogt, P.R., 1979. Western North Atlantic: sedimentary evolution and aspects of tectonic history. Initial Rep. Deep Sea Drill. Proj. 43, 791–826.
Via, R.K., Thomas, D.J., 2006. Evolution of Atlantic thermohaline circulation: Early Oligocene onset of deep-water production in the North Atlantic. Geology 34, 441–444.
Voigt, S., Gale, A.S., Jung, C., Jenkyns, H.C., 2012. Global correlation of Upper Campanian–Maastrichtian successions using carbon-isotope stratigraphy: development of a new Maastrichtian timescale. Newslett. Stratigr. 45, 25–53.
Wang, Y.L., Liu, Y.-G., Schmidt, R.A., 1986. The geochemistry of rare earth elements in South Atlantic deep sea sediments; Ce anomaly changes at 54 My. Geochim. Cosmochim. Acta 50, 1337–1356.
Zachos, J.C., Dickens, G.R., Zeebe, R.E., 2008. An early Cenozoic perspective on greenhouse warming and carbon-cycle dynamics. Nature 451, 279–283.
Zepeda, M.A., 1998. Planktonic foraminiferal diversity, equitability and biostratigraphy of the uppermost Campanian–Maastrichtian, ODP Leg 122, Hole 762C, Exmouth Plateau, NW Australia, eastern Indian Ocean. Cretaceous Res. 19, 117–152.